ELSEVIER

Carbohydrate Polymers 37 (1998) 25–39

Carbohydrate Polymers

Conformational analysis of galactomannans: from oligomeric segments to polymeric chains

C. L. O. Petkowicz[a], F. Reicher[a], K. Mazeau[b,*]

[a]*Departamento de Bioquimica, CP 19046, UFPR, 81531-990 Curitiba, Brazil*
[b]*CERMAV, CNRS, Université J. Fourier, BP 53, 38041 Grenoble Cedex 9, France*

Received 18 October 1997; revised 24 March 1998; accepted 22 April 1998

Abstract

Conformational features of the glycosidic bond linking two mannosyl units of four different oligomeric fragments of galactomannans have been calculated by means of adiabatic mapping of the glycosidic Φ, Ψ torsion angles using the MM3 force field. These fragments differed in their substitution pattern. The aim of this study was to ascertain the role played by the galactosyl side groups on the conformational flexibility of the galactomannan chain backbone. Although the overall features of all the potential energy surfaces created appear similar, these maps show that the position of the lowest energy minimum conformer and the lower energy region change significantly if one or both mannosyl residues are substituted by a galactosyl side group. Thus, these groups lead to significant differences in the accessible conformational space, when compared with that of the mannobiose molecule. Predicted homonuclear and heteronuclear coupling constants averaged over each entire map also reflect the conformational differences.

Computed maps were used to predict polymeric unperturbed dimensions, C_∞, a, $\langle R \rangle$ and $\langle s^2 \rangle^{1/2}$ of idealized galactomannan chains by Monte Carlo methods. For low values of Man:Gal ratios, chain extension appears to be strongly dependent on the degree of substitution. For 2:1 and 3:1 Man:Gal ratios, random, alternate and block patterns of substitution have been investigated. It has also been shown that the spatial extension of the polymer chains is dependent on the scheme of substitution. Such studies provide a unique insight into the dependence of these two factors on the stiffness and flexibility of different galactomannan chains.

Keywords: Galactomannans; Oligomeric segments; Polymeric chains

1. Introduction

Endosperm seed galactomannans are storage polysaccharides having a linear backbone of β-(1 → 4) linked D-mannose units, to which various amounts of single α-(1 → 6)-linked D-galactose residues are attached (between 5% and 100%). Their structural and physico-chemical characteristics depend on the plant source and on the extraction conditions (Reid & Edwards, 1995, Izydorczyk & Biliaderis, 1996). These hydrocolloids are widely used as thickening agents in the food industry, as well as having uses in many other industrial sectors (Reid & Edwards, 1995). In addition, chemically modified naturally occurring galactomannans display unique features in novel applications (Lapasin et al., 1995, Ahuja & Rai, 1997).

The importance of galactomannans in industry makes them an interesting subject for physico-chemical studies (Garnier et al., 1995, Viebke & Piculell, 1996, Craig et al., 1997, Sudhakar et al., 1996). Since galactomannan samples differ according to their galactose content and distribution, and their fine structure seems to depend on their botanical source, they provide a challenging and complex topic for investigation. However, the experimental correlation between chemical structure and solution properties is extremely difficult to establish. The distribution of galactose side groups along the mannan backbone has been shown to be near random, alternately disposed or in blocks. However, their true structure remains unknown (Hall & Yalpani, 1980, McCleary et al., 1985, Hoffman & Svensson, 1978, Grasdalen & Painter, 1980, Painter et al., 1979).

Side chain content and distribution are likely to influence the solution properties of galactomannans (Reid & Edwards, 1995, Viebke & Piculell, 1996). Experimental and theoretical studies have considered the conformational features of oligomeric segments of galactomannans in an attempt to explain the geometric and energetic effects of the galactosyl substitution on the main chain flexibility (Bergamini et al., 1995). Theoretical calculations of solution conformations of mannobiose have been reported in the literature (Tvaroska et al., 1987, Jimenez-Barbero et al., 1988). It has been

* Corresponding author

0144–8617/98/$ - see front matter
PII S0144-8617(98)00051-4

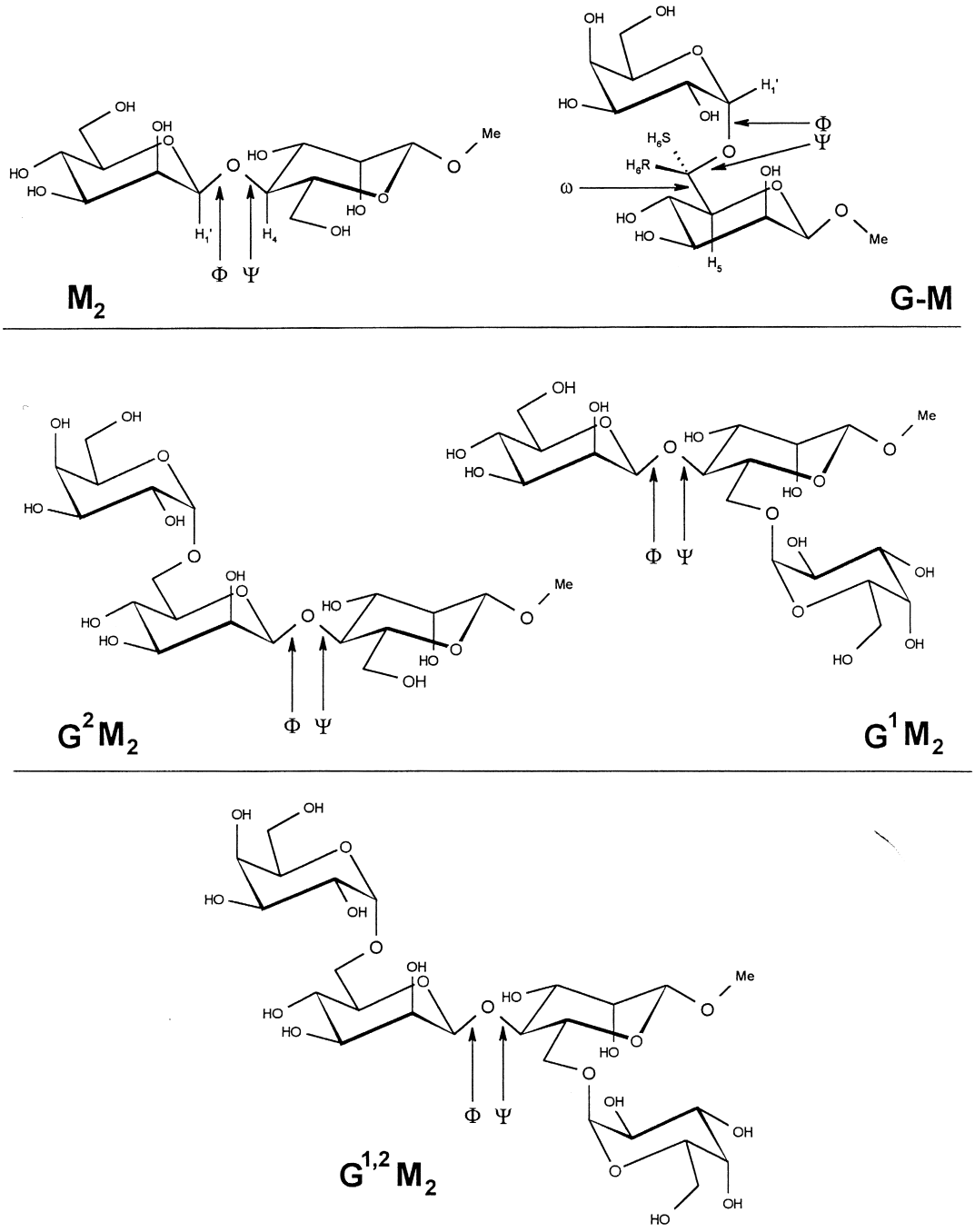

Fig. 1. Schematic representation of oligomeric fragments occurring in galactomannan chains.

shown that, in the isolated state, a conformational equilibrium between seven conformers could occur, as calculated by the semi-empirical PCILO method. Evaluation of the solvation effect using a continuum approach suggests that the relative abundance of the conformers is influenced by the solvent polarity. The most stable conformer predicted in the isolated state is stabilized by a bifurcated hydrogen bond between O-3H, O-5′ and O-2′, and its population increases with an increase in solvent polarity (Tvaroska et al., 1987). Conformational analysis by molecular modelling and nuclear magnetic resonance spectroscopy (NMR) of the two dimeric segments of galactomannan chains was recently described by Bergamini et al. (1995). The existence of three types of helices of unsubstituted mannan chains were predicted based on the stable conformers of the parent disaccharide. It was shown that the introduction of galactose residues resulted in either a large or an insignificant distortion compared to the native helices. Furthermore, random-coil conformations of a backbone chain of ten residues in length were generated, the results show that the limiting structures are either very extended or compact. Substitution of mannosyl units by galactosyl groups leads to a local

bending of the backbone, the geometry of which is stabilized by non-bonding interactions. However, these data do not reveal the effect of the substitution on the flexibility of the mannan chain.

Using molecular mechanics and Monte Carlo methods, the present study addresses the role of galactosyl substitution on the flexibility and spatial extension of the mannan backbone and discusses how the different patterns of substitution affect the average parameters such as the NMR coupling constants of representative oligomeric segments and the characteristic ratio and persistence length of polymeric chains.

2. Materials and methods

Fig. 1 shows a schematic representation of the five oligomers that represent all the combinations of primary structures that could occur in native galactomannan chains. Two disaccharides represent the basic repeating units: 4-*O*-*β*-D-mannopyranosyl-D-mannose, having the trivial name mannobiose (Fig. 1*a*) denoted by M_2 in this study and 6-*O*-*α*-D-galactopyranosyl-D-mannose or epimelibiose (Fig. 1*b*), denoted by G-M. M_2 represents the unsubstituted mannan backbone, while the conformational investigation of G-M is necessary to characterize the relative low-energy orientations of the side chain (galactosyl group) with respect to the mannan chain. However, three other oligosaccharides should be considered: two trimers where the mannobiose is substituted by a galactose either on the reducing end, *O*-*β*-D-mannopyranosyl-(1 → 4)-[*O*-*α*-D-galactopyranosyl-(1 → 6)]-D-mannose (G^1M_2) (Fig. 1*c*), or on the non-reducing end, *O*-*α*-D-galactopyranosyl-(1 → 6)-*O*-*β*-D-mannopyranosyl-(1 → 4)-D-mannose (G^2M_2) (Fig. 1*d*). The latter structure is a tetramer, in which the mannobiose is fully substituted: *O*-*α*-D-galactopyranosyl-(1 → 6)-*O*-*β*-D-mannopyranosyl-(1 → 4)-[*O*-*α*-D-galactopyranosyl-(1 → 6)]-D-mannose 6^1-galactosyl-mannobiose ($G^{1,2}M_2$) (Fig. 1*e*).

The conventions proposed by the Commission on Nomenclature IUPAC (1989), IUPAC-IUB (1997) are used throughout this paper. For (1 → 4) glycosidic linkages, the torsion angles that describe the orientation of two consecutive mannosyl units, are defined by: Φ = O-5′–C-1′–O-4–C-4 and Ψ = C-1′–O-4–C-4–C-5. The primed atoms correspond to the non-reducing residue and the unprimed atoms correspond to the reducing one. Other torsion angles of interest are Φ_H = H-1′–C-1′–O-4–C-4 and Ψ_H = C-1′–O-4–C-4–H-4, which characterize the conformation around the glycosidic bonds and allow the computation of the NMR coupling constants. The orientation around the C-5–C-6 bond is defined by ω = O-5–C-5–C-6–O-6. For the graphical representation of all oligomers, the starting geometries of the monomeric units were derived from the library of the software package QUANTA (Molecular Simulation, Inc.).

The mannobiosyl conformational space of each oligomer was explored in a systematic fashion by stepping the glycosidic Φ and Ψ torsion angles in 10° increments over the whole angular range. At each conformational microstate a geometry optimization was performed by allowing the coordinates of each atom to vary except those defining the Φ and Ψ torsion angles. The results from this procedure are presented as Ramachandran-like contour plots and referred to as relaxed (Φ, Ψ) maps. Because of the well-known multiple-minima problem of the potential-energy hypersurface due to the large number of degrees of freedom, together with the inherent limitations of the minimization procedures, emphasis is placed on the importance of drawing adiabatic maps by using starting geometries with different orientations of the pendant groups. Adiabatic maps were plotted by taking into account the lowest energy conformer at each (Φ, Ψ) point. Thus, for both the dimeric fragments (mannobiose and epimelibiose) the main factors taken into consideration were: (1) all the possible staggered combinations ($-60°$, 60° and 180° usually referred as *gg*, *gt* and *tg*, respectively) of both ω torsion angles, and (2) the approximation concerning the three possible hydrogen-bonding networks (clockwise and counter-clockwise) that are created by the orientations of the secondary hydroxyl groups on atoms C-2, C-3 and C-4 (non-reducing unit) around each ring. The adiabatic maps of both M_2 and G-M were then created from 36 different orientations of the pendant groups. Computation of the Φ, Ψ adiabatic maps of the trimeric and tetrameric fragments were achieved by using the same procedure. Galactosyl groups attached to the mannobiosyl molecule were considered as pendant groups, and only the optimized geometry of the three lowest energy minima of the adiabatic study of epimelibiose were taken into account. For the computation of the adiabatic maps 48, 48 and 64 starting conformations of G^1M_2, G^2M_2, and $G^{1,2}M_2$ were used, respectively. The iso-energy contours were drawn by interpolation of the 1 kcal mol^{-1} contour and the 10 kcal mol^{-1} contour was selected as the outer limit. Contoured maps were generated using CARTO, an in-house software program.

Geometry optimization was performed using the molecular mechanics program MM3(92) (Allinger et al., 1989, 1992). The MM3 force field contains a correction for the anomeric effect and has been specially adapted for the study of carbohydrates (Dowd et al., 1992–1995, French et al., 1997). The block-diagonal minimization method, with the default energy convergence criterion of 0.00008**n* kcal mol^{-1} per five iterations (*n* being the number of atoms) was used for grid point optimization. In order to mimic the solvation effects, a dielectric constant, $\varepsilon = 80$, was used in all the calculations.

From the predicted geometries for each conformational state, theoretical NMR coupling constants can be estimated by using the appropriate Karplus-type equations. The geometrical parameters of interest are the H-C-C-H torsion angles for homonuclear couplings and the interglycosidic H-C-O-C (Φ_H and Ψ_H) torsion angles for heteronuclear carbon-proton couplings. The equations describing the angular dependence of the coupling constants are those of Haasnoot et al. (1980) for homonuclear coupling constants

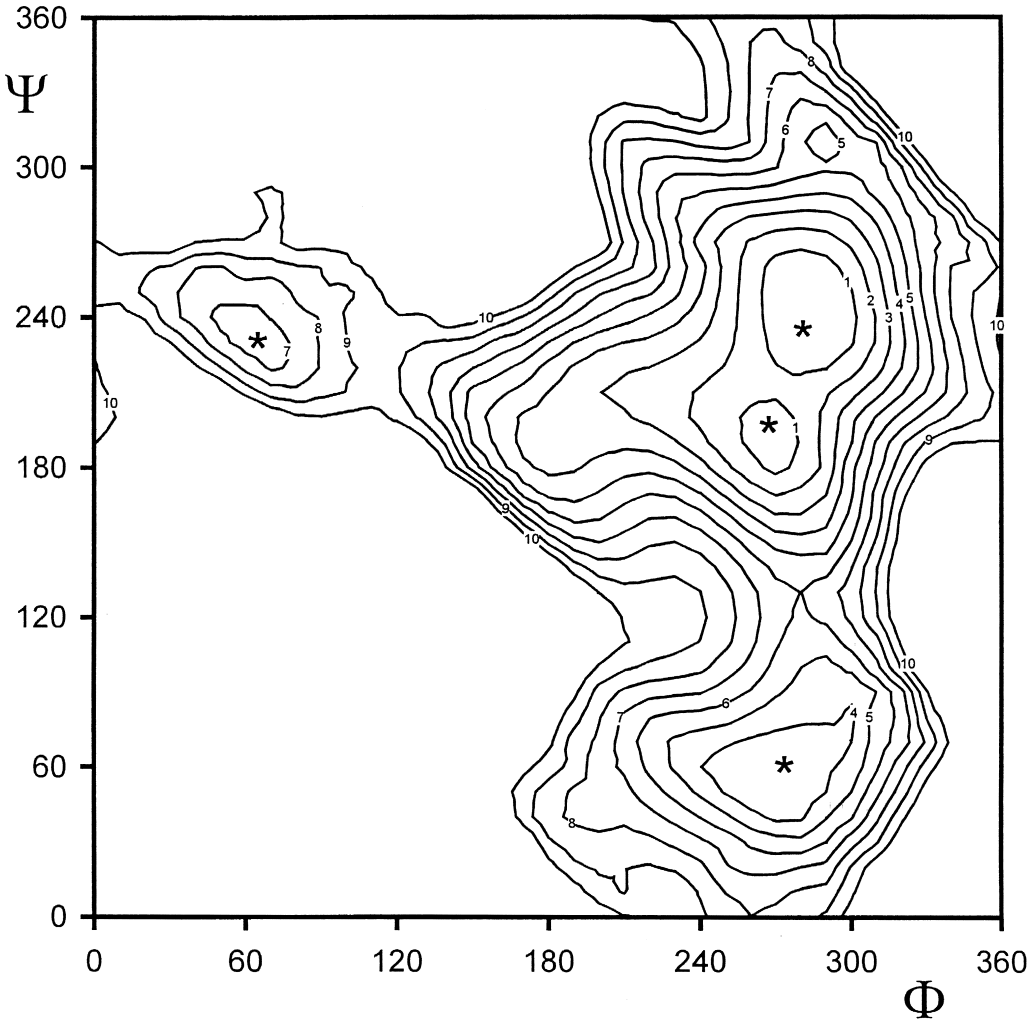

Fig. 2. MM3 adiabatic potential energy surface of the M_2 disaccharide as a function of the Φ and Ψ torsion angles (* locates the energy-minima).

and Tvaroska et al. (1989, 1991, 1992) for the heteronuclear coupling constants. The ensemble average coupling constant $\langle J \rangle$ is given by

$$\langle J \rangle = \sum P_i J_i$$

Where P_i is the normalized Boltzmann abundance of the conformer i and J_i its corresponding coupling constant.

From the adiabatic energy surfaces, normalized Boltzmann abundances of each Φi, Ψi conformational micro-state at 50°C could be calculated. Subsequently, 4000 galactomannan chains having a degree of polymerization of 3000 each, were generated according to the Metropolis Monte-Carlo (MMC) procedure (Metropolis et al., 1953). First, to address the question of the effect of the degree of substitution on chain dimensions, unsubstituted mannan chains were generated, as well as substituted ones having different Man:Gal ratios of 1:1, 2:1, 3:1, 4:1 and 5:1. These 2:1, 3:1, 4:1 and 5:1 chains were initially generated assuming a random distribution of the substituents. Second, to study the influence of the primary structure on the calculated mean chain dimensions, similar simulations were carried out for different models of galactomannan chains, having Man:Gal ratios of 2:1 and 3:1, and differing in their substitution patterns. These patterns of substitution were random, alternate and by blocks. The block size for 2:1 galactomannan was five and they were constructed with six non substituted mannose units attached to three contiguous substituted residues for 3:1 polymers.

This configurational sampling allowed the calculation of the unperturbed dimensions of the different chains using the in-house program Metropol. A complete description of the program has been provided (Boutherin et al., 1997). Here, only an outline of the method will be presented.

The mean spatial characteristics of the different chains can be described by the mean square radius of gyration $\langle S^2 \rangle^{1/2}$ which is defined as the *rms* distance of a segment from its common centre of gravity. It is calculated as follows $\langle S^2 \rangle^{1/2} = 1/X^2 \Sigma \langle R_{ij} \rangle$ where X is the degree of polymerization and R_{ij} is the vector from bead i to bead j. The characteristic ratio $C_\infty = \lim C_x = \lim \langle R^2 \rangle / XL^2$, is a

Table 1
Calculated Φ, Ψ torsion angles for β-(1 → 4) linkage, ω angles, energy and dipolar moment of minima for M_2, G^1M_2, G^2M_2 and $G^{1,2}M_2$ oligomers

	Φ (degree)	Ψ (degree)	ω_M (degree)	$\omega_{M'}$ (degree)	ω_{G1} (degree)	ω_{G2} (degree)	E (kcal mol^{-1})	ΔE (kcal mol^{-1})	μ (D)
M_2									
M_2-1	282	240	295	68	–	–	30.17	0.00	6.13
M_2-2	269	191	294	69	–	–	30.62	0.45	3.46
M_2-3	272	58	70	69	–	–	33.18	3.01	7.95
M_2-4	295	304	71	68	–	–	34.30	4.13	9.20
M_2-5	66	233	65	68	–	–	36.42	6.25	4.34
G^1M_2									
G^1M_2-1	269	196	57	67	71	–	36.53	0.00	5.83
G^1M_2-2	280	59	77	295	71	–	37.58	1.05	4.74
G^1M_2-3	291	90	57	76	68	–	38.11	1.58	3.02
G^1M_2-4	294	304	82	294	80	–	39.82	3.29	4.25
G^1M_2-5	58	233	68	181	73	–	41.29	4.76	3.97
G^1M_2-6	68	82	62	182	74	–	45.71	9.18	7.11
G^2M_2									
G^2M_2-1	290	240	65	75	–	72	34.86	0.00	4.17
G^2M_2-2	290	80	62	71	–	73	36.84	1.98	4.59
G^2M_2-3	301	306	67	63	–	72	40.06	5.20	2.21
G^2M_2-4	180	189	65	73	–	69	40.87	6.01	6.37
G^2M_2-5	53	237	63	76	–	68	43.66	8.80	6.62
$G^{1,2}M_2$									
$G^{1,2}M_2$-1	288	230	75	64	72	72	44.74	0.00	5.43
$G^{1,2}M_2$-2	278	54	60	62	73	71	45.16	0.42	4.17
$G^{1,2}M_2$-3	308	292	70	57	72	66	47.82	3.08	5.99
$G^{1,2}M_2$-4	49	239	70	64	70	73	50.42	6.08	5.35

dimensionless quantity in which C_x corresponds to the mean-square end-to-end length of the chain $\langle R^2 \rangle$ normalized by the number X of sugar residues in the chain and L, the virtual bond connecting adjacent glycosidic oxygens. In our study L was taken as 5.44 Å, which is the average value computed from the oligomeric potential energy surfaces. Similarly, the magnitude of the persistence length, a, can be evaluated by using $a = \lim L_x$, where L_x represents the average projection of the end-to-end distance vector on the first bond of the chain in the limit of infinite chain length; it indicates the distance through which the chain can be considered as linear.

All calculations were carried out on a Silicon Graphics Indigo workstation and on the parallel computer (SP2) at the Centre National Universitaire Sud de Calcul-Montpellier-France.

3. Results and discussion

3.1. Unsubstituted disaccharides

The profile of the adiabatic map for the M_2 disaccharide is shown in Fig. 2. As generally found for equatorially–equatorially linked disaccharides, such as sophorose, laminarabiose and cellobiose (Dowd et al., 1992, French, 1989), the map has two perpendicular intersecting low-energy axes. Favourable conformations of the Φ torsion angle occur mainly at values around 300° (− *gauche*) while minor conformations experience a range of 60° (+ *gauche*). This is in good agreement with the exo-anomeric effect (Tvaroska & Kozar, 1980) which favours the *gauche* orientations of the glycosidic C-1–O bond aglycone.

Presented in Table 1 are selected geometrical parameters along with the energies of the different minima. The two lowest energy minima, M_2-1 and M_2-2, were found within the same potential energy well. Following complete optimization, they were located at Φ, Ψ values of (282°, 240°) and (269°, 191°), respectively. These values are very close to those determined in the solid state (Sheldrick et al., 1984). An energy difference of only 0.5 kcal mol^{-1} existed between the two minima. The lowest energy conformer is stabilized by an O-3(H)–O-5′ inter-residue hydrogen bond with an oxygen–oxygen distance of 2.9 Å. Another three additional minima were observed, two of these, M_2-3, at (272°, 58°) and M_2-4 at (295°, 304°) were found to be aligned along the same Φ axis as that of M_2-1 and M_2-2. M_2-5 with Φ torsion angle in the + *gauche* orientation, angle (66°, 233°) is higher in energy by 6.3 kcal mol^{-1}. A combination of NMR spectroscopy and molecular modelling (using solvation effects) on the mannobiose, has established that the conformation M_2-5 is dominant (Bergamini et al., 1995) in water solution. The preferred orientation of the M_2 energy minima's hydroxymethyl groups in the two

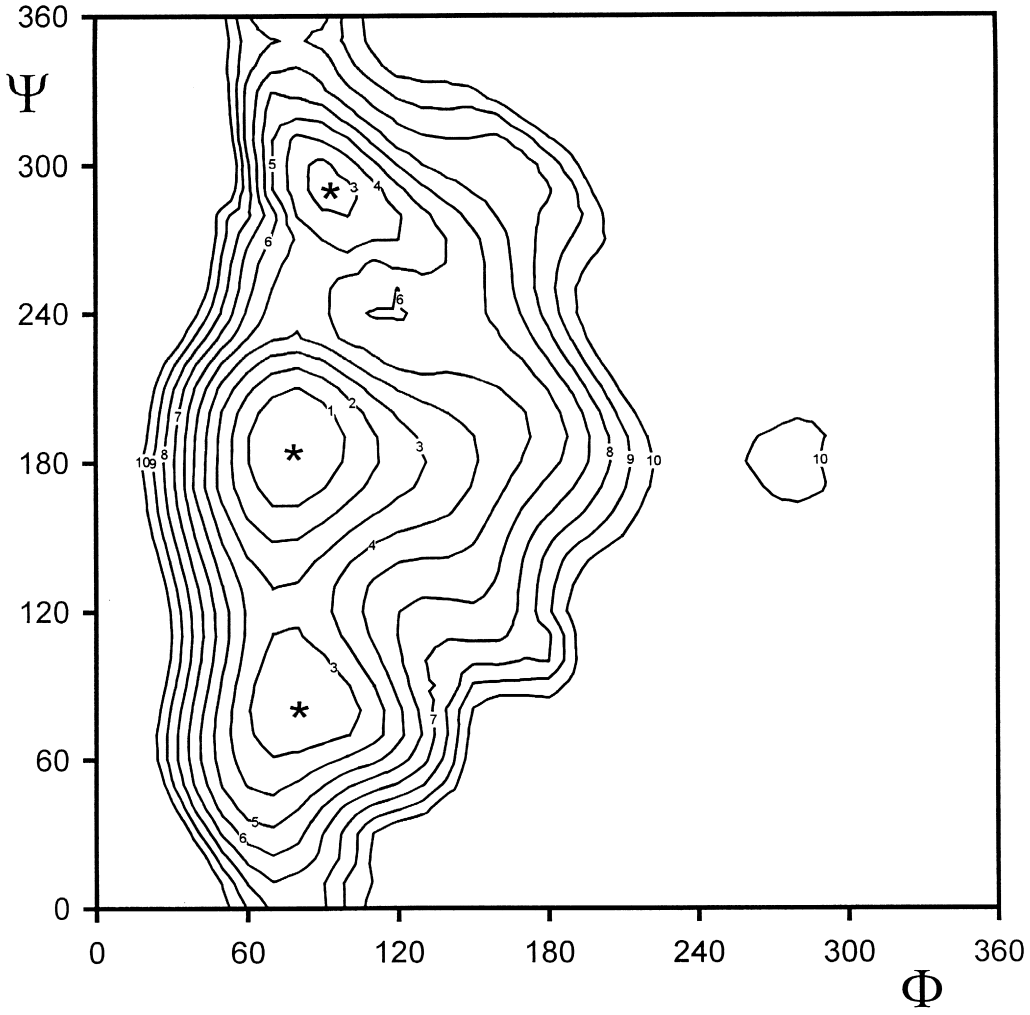

Fig. 3. MM3 adiabatic potential energy surface of the G-M disaccharide as a function of the Φ and Ψ torsion angles (* locates the energy-minima).

lowest energy conformers was *gg* on the reducing monomer. However, on the non-reducing end, the *gt* orientation is preferred. All the others conformers would prefer the *gt* orientation of both pendant groups. From the whole potential-energy surface, the hydroxymethyl group on the reducing monomer has preferentially a *gg* orientation (62% of the surface), whereas on the non-reducing end, 77% of the surface corresponds to a *gt* orientation.

For the G-M disaccharide the adiabatic map is given in Fig. 3. This map may be compared with the MM3 relaxed-map of Bergamini et al. (1995). Both surfaces are similar and the minor differences observed may be accounted for by the use of different dielectric constant values and starting geometries. A low energy region extending along the Ψ axis was observed which corresponds to the + *gauche* staggered orientation of the Φ torsion angle. This is in agreement with the exo-anomeric effect reported by Tvaroska & Kozar (1980). The *trans* orientation (180°) did not correspond to the energy minimum and the − *gauche* conformer was found at higher energy regions. The Ψ torsion angle displayed different behaviour because all three staggered orientations were stable. Values of around − 60° had considerably higher energy than those at 60° and 180°. Thus, such conformations would not be represented in the equilibrium mixture.

Four low-energy areas were identified on the above surface. The lowest energy conformer was observed at Φ, Ψ values of (79°, 192°). This position is in agreement with the lowest energy conformer of G-M as determined by Bergamini et al. (1995) using quantum chemical methods. Other minima occurred at (79°, 83°); (87°, 293°) and (129°, 242°); with energies of 1.8, 2.2 and 5.9 kcal mol^{-1}, respectively, above the calculated *minimum minimorum*. The *gt* orientation of the hydroxymethyl group of galactose was preferred for all the six minima, as expected, because of the axial oxygen on the C-4 atom (Marchessault & Perez, 1979). Although, for galacto-type residues, it is generally accepted that the *tg* conformation is favoured, our results indicated that the *tg* population is poorly represented with just 3.2% of the total surface. The glycosidic linkage torsion

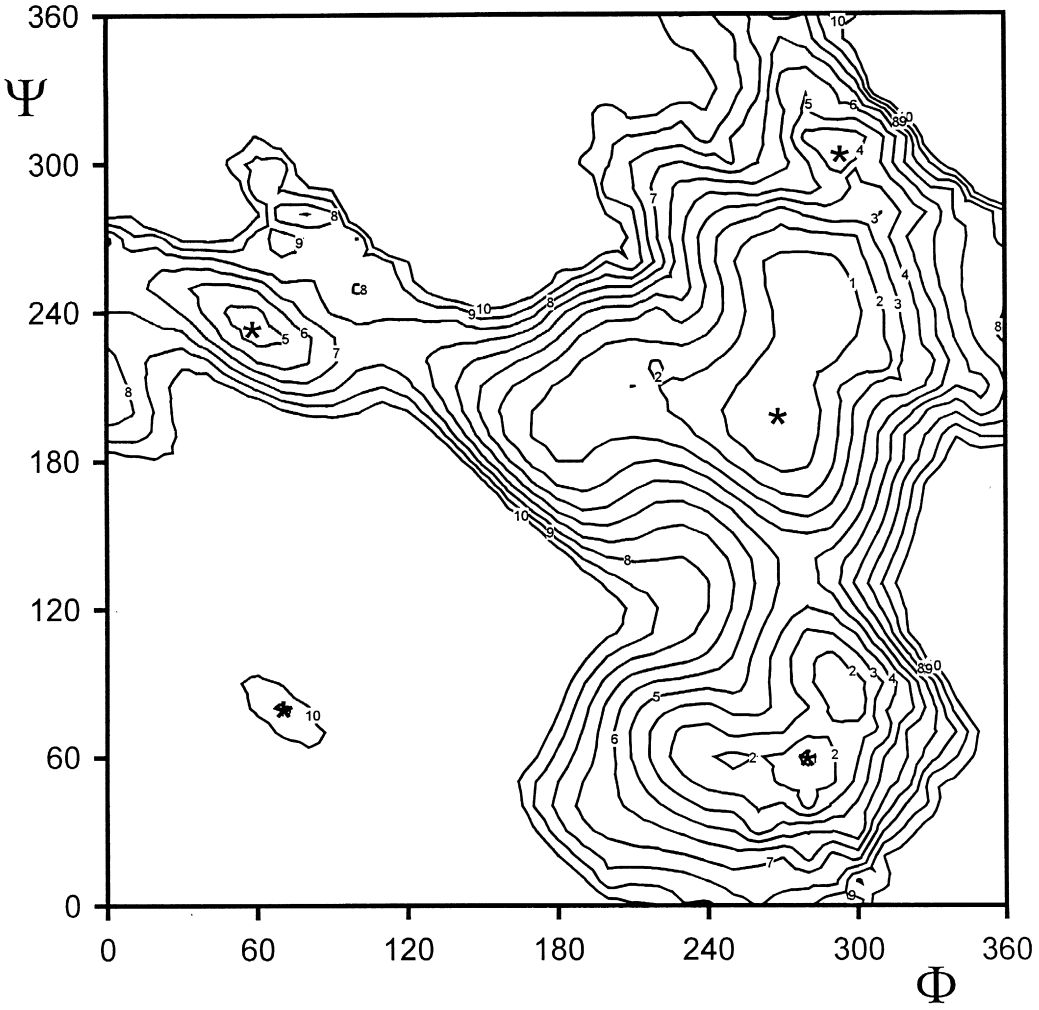

Fig. 4. MM3 adiabatic potential energy surface of the G^1M_2 trisaccharide as a function of the Φ and Ψ torsion angles (* locates the energy-minima).

angle was also found to correspond principally to the *gt* conformation (67%). The present results show that the conformations of the G-M disaccharide can be properly described by four structures in equilibrium with (Φ, Ψ, ω) values of (79°, 192°, 74°), (79°, 83°, 71°); (87°, 293°, 79°) and (129°, 242°, 72°). All of these were used in the computation of the maps corresponding to the trimers and tetramer.

3.2. Effect of substitution

A galactosyl side chain on the reducing or non-reducing end of the M_2 disaccharide gave compounds G^1M_2 and G^2M_2, whose adiabatic conformational energy surfaces are presented in Figs. 4 and 5, respectively. Fig. 6 shows the calculated contour map obtained by simultaneous introduction of a galactosyl side chain on both monomers of M_2 (compound $G^{1,2}M_2$). Values of the key torsion angles Φ, Ψ and ω for the different residues, along with dipole moments (μ) and energies of the predicted minima for the four oligomers studied are listed in Table 1. A molecular drawing of each of the lowest energy conformers is shown in Fig. 7.

Each map created displayed a similar shape. The accessible values of the torsion angles Φ and Ψ around the glycosidic bond of the mannobiose part for different molecules appear to be equivalent. However, specific details of each map should reflect the effect of different schemes of substitution. Other differences such as the position of the lowest energy conformer, the number and energies of observed minima, and different barrier heights between minima may also be found.

The total accessible space, delimited by the 10 kcal mol^{-1} limit, was equivalent for G^1M_2 and M_2. This suggests qualitatively that the substitution of the hydroxymethyl side group by the galactosyl group on the reducing manosyl unit have only a slight influence on the overall flexibility. However, the total accessible surface of G^2M_2 and $G^{1,2}M_2$ was considerably lower than that of M_2, resulting in a general lowering of flexibility. This result indicates that the substitution on the non-reducing unit has the more significant

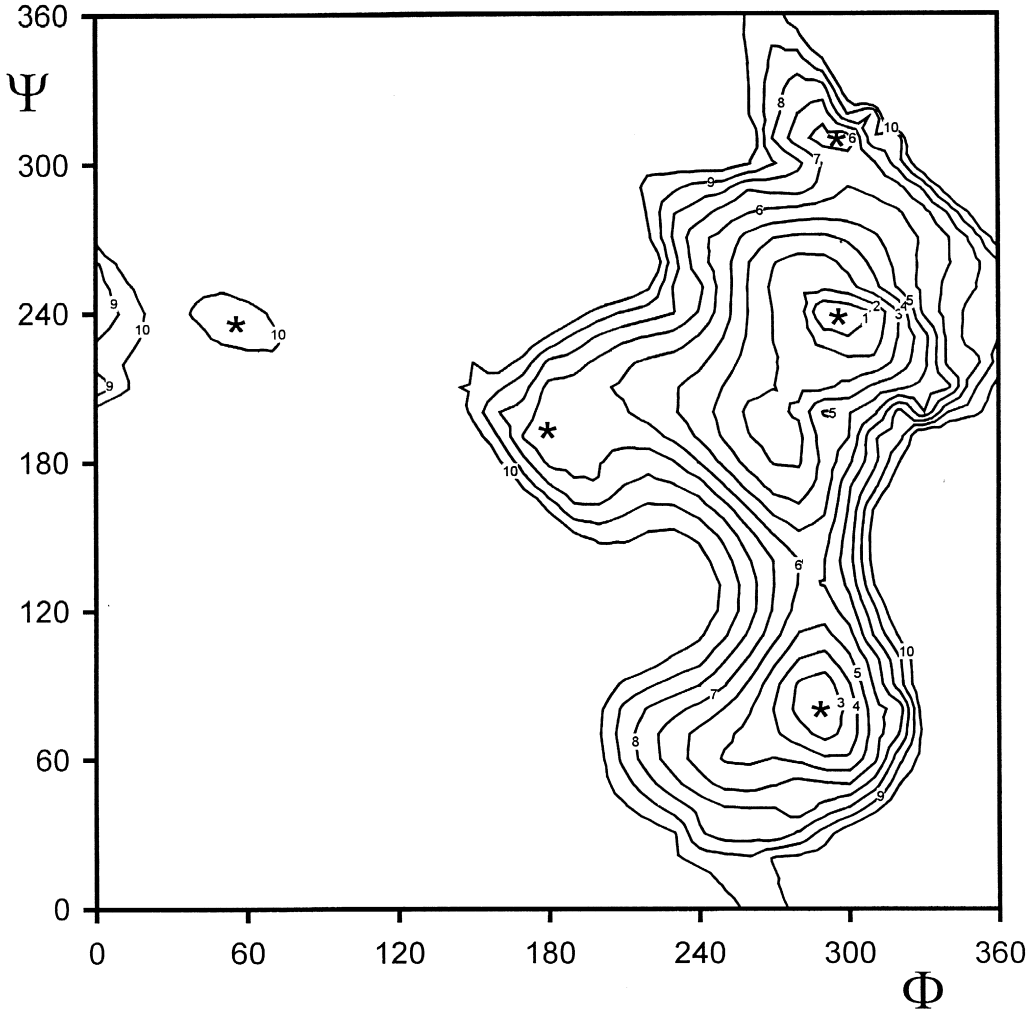

Fig. 5. MM3 adiabatic potential energy surface of the G^2M_2 trisaccharide as a function of the Φ and Ψ torsion angles (* locates the energy-minima).

influence on the flexibility of the glycosidic linkage between the two mannoses.

The lowest energy contours of the maps computed for the substituted oligomers displayed remarkable differences when compared with those computed for the unsubstituted oligomer. Evidence suggests that the principal region for the M_2 map is shallow, with multiple equivalent conformers. This region showed unambiguously, two large low-energy spaces that are separated by an energy barrier higher than 1 kcal mol^{-1}. Thus, conformational fluctuations and interconversions may occur. Maps of the substituted oligomers displayed a steep first contour, suggesting an extra-stabilization of one particular conformation (the lowest energy minima of M_2 for G^1M_2 or the second lowest conformer of M_2 for G^2M_2 and $G^{1,2}M^2$) as compared to all the other conformers within this region. In this case, the libration motion around the exact position of the minimum appeared to be very restricted.

This behaviour was not the same as for the auxiliary region at Φ, Ψ values of approximately (270°, 60°). Low-energy conformers were encompassed by the fifth contour in the M_2 case, whereas for the others compounds they were encompassed by the third. Within this area only one conformer was observed for M_2 and G^2M_2. This minimum had little influence over the global map of M_2 as its relative energy is higher than that of the global minimum (3 kcal mol^{-1}) but should be more important in the substituted oligomers because their relative energies are 1 kcal mol^{-1}, 2 kcal mol^{-1} and 0.5 kcal mol^{-1} for G^1M_2, G^2M_2 and $G^{1,2}M_2$, respectively. However, for G^1M_2 and $G^{1,2}M_2$ three conformers were clearly distinguishable suggesting an enhanced flexibility for these compounds in this region. The remaining stable area of the maps was located at Φ, Ψ values of around (60°, 240°). For G^2M_2 and $G^{1,2}M_2$, this region is deepened with respect to M_2, and G^1M_2 (which is absent in the G^1M_2 map).

The results of this study show that the location of the substitution influences the overall flexibility of the glycosidic bond for mannobiose. A quantitative estimate of the

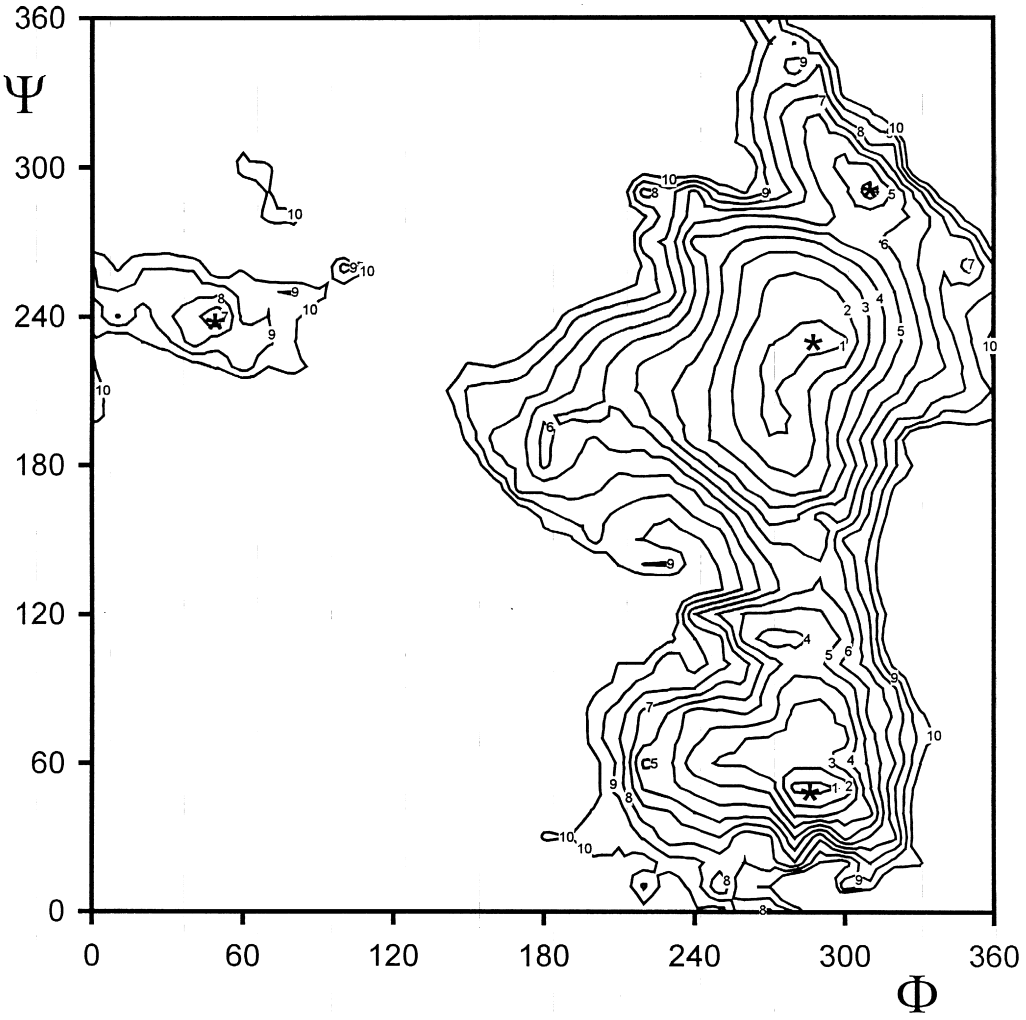

Fig. 6. MM3 adiabatic potential energy surface of the $G^{1,2}M_2$ tetrasaccharide as a function of the Φ and Ψ torsion angles (* locates the energy-minima).

conformational freedom of the glycosidic linkages is given by the calculated partition function (**q**). For M_2, **q** had a value of 66 deg^2. Galactosyl substitution on the reducing end of mannobiose increased **q** to 97 deg^2 whereas on the non-reducing residue decreased it to 4 deg^2. Disubstituted mannobiose compound had a **q** value of 17 deg^2. Therefore, compared to M_2, G^1M_2 is very flexible, whereas G^2M_2 and $G^{1,2}M_2$ are not. Concerning the lowest energy area, substituted oligomers had a very restricted libration motion and the interconversions between different minima required surmounting a high energy barrier. This also strongly favours the extra-stabilization of a few particular conformers.

Changes in flexibility with the substitution may be due to the steric interaction imposed by the presence of bulky side-groups, as compared to the hydroxymethyl group. However, because of the presence of numerous hydroxyl groups, some conformers are stabilized by hydrogen bonding between the galactosyl side group and the mannosyl residues. Note that this phenomenon was observed despite the use of a dielectric value of 80 which, in principle, should decrease the importance of electrostatic interactions. Inspection of the oxygen–oxygen distances of the lowest energy minimum of each map suggested that hydrogen bonding occurs within these structures. The combination of the Φ and Ψ torsion angles between the two mannoses allows these residues to interact with the hydroxyl group HO-3 through the oxygen atom O-5′. In addition to this common feature, structures G^2M_2 and $G^{1,2}M_2$ are stabilized by hydrogen bonding between distant residues. All of them involve the HO-3 group of the reducing mannose and the HO-6 and HO-2 groups of the galactose carried by the non-reducing mannose. These hydrogen bonds are characterized by an average oxygen–oxygen distance of 2.9 Å.

Predicted values of observable NMR parameters, computed by proper averaging over the entire maps, also indicated conformational differences between all the calculated structures. The key coupling constants which are frequently used in conformational analysis of

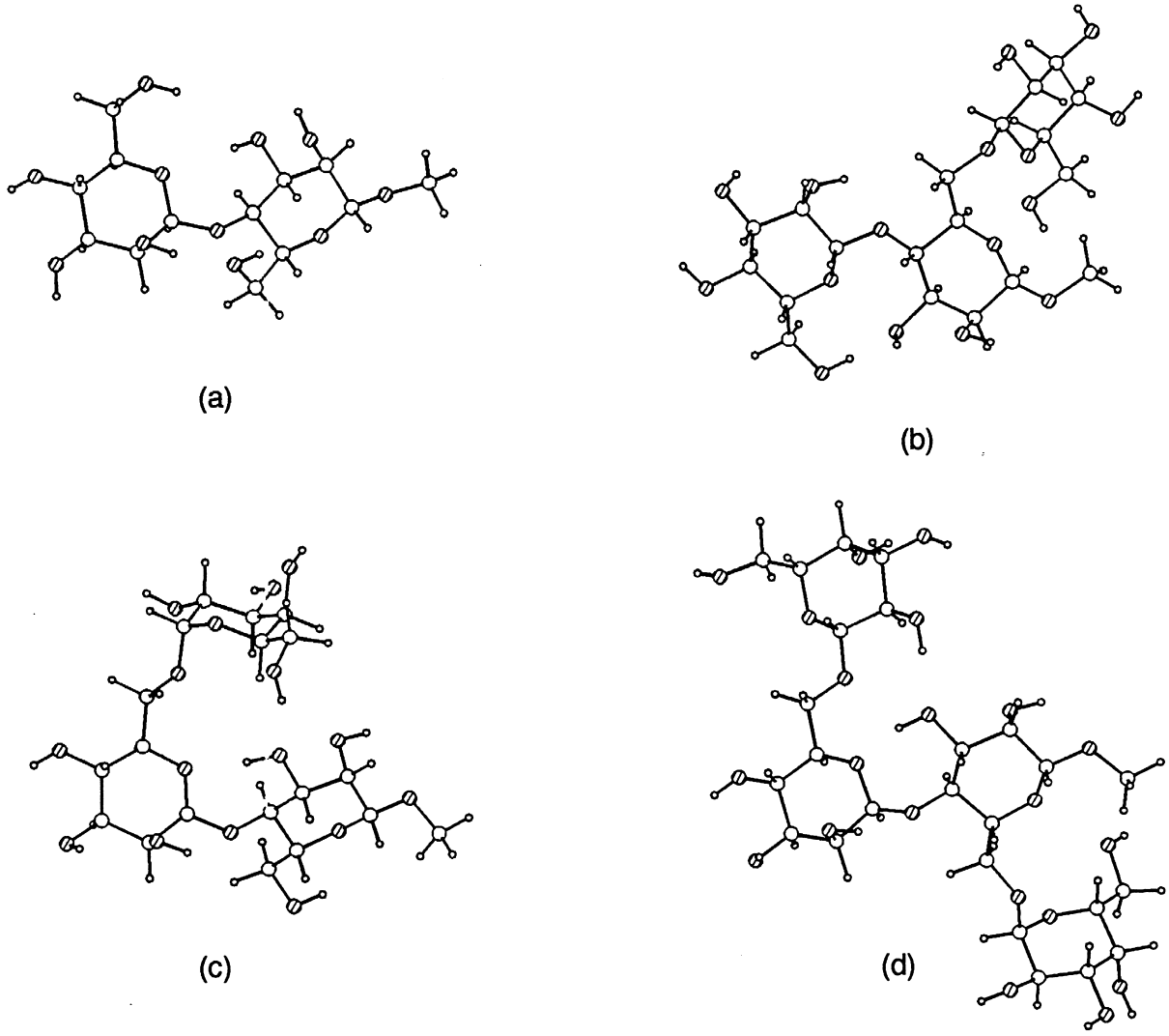

Fig. 7. Molecular representations of the lowest energy conformers of M_2 (a), G^1M_2 (b), G^2M_2 (c) and $G^{1,2}M_2$ (d).

carbohydrates are those measured through the glycosidic bonds (Taravel et al., 1995); they are reported in Table 2. Calculated carbon-proton coupling constants for M_2 (Table 2) show a reasonable agreement with already known experimental values (Bergamini et al., 1995). It is clear, by inspection of Table 2, that the sensitivity of these parameters differ. Heteronuclear three-bond carbon-proton couplings show substantial variations and they are, thus, the most sensitive parameter, while heteronuclear one-bond couplings differ by less than 0.5 Hz. The large differences observed for the $^3J_{CH}$ couplings between the two mannoses stresses that both Φ and Ψ torsion angles are sensitive to galactosyl substitution. Note that such behaviour has also been measured by NMR spectroscopy (Bergamini et al., 1995). A $^3J_{H1'\text{-}C4}$ difference of 0.4 Hz has been reported between M_2 and G^2M_2 while the measured $^1J_{CH}$ were almost identical. While larger, our predicted difference is in agreement with the measured values. The glycosidic bridge between a galactosyl group and the mannose have three rotatable bonds. Therefore three variables, namely Φ, Ψ and ω are necessary to define the average glycosidic geometry. The first two are properly described by $^3J_{CH}$ coupling between C-6 and H-1 (angle Φ), and C1 and H-6_R or H-6_S for the Ψ angle. The angle ω is dependent on the homonuclear $^3J_{HH}$ between H-5 and H-6_R or H-6_S. It is obvious from inspection of Table 2 that the different segments studied principally accommodate the substitution by variation of the Ψ torsion angle.

3.3. Polymer chain characteristics

From the potential energy surfaces of appropriate skeletal segments of galactomannan chains, 4000 samples of galactomannan having 3000 backbone residues each were generated according to the MMC procedure. In this simulation different substitution rates were investigated ranging from a pure unsubstituted mannan chain (Man:Gal ratio of

Table 2
Calculated $^{1}J_{C\text{-}H}$, $^{3}J_{C\text{-}H}$ and $^{3}J_{H\text{-}H}$ coupling constants (Hz)

Coupling	M_2	G-M	G^1M_2	G^2M_2	$G^{1,2}M_2$
$^{1}J_{C\text{-}H}$					
C1-H1(M′)	162.5	–	162.5	162.6	162.6
C1-H1(G1)	–	169.8	169.5	-	169.4
C1-H1(G2)	–	–	–	169.7	169.5
C4-H4(M)	146.5	–	146.7	146.5	146.8
C6-H6R(M)	–	146.4	148.3	–	146.5
C6-H6S(M)	–	146.6	146.4	–	146.5
C6-H6R(M′)	–	–	–	146.6	147.7
C6-H6S(M′)	–	–	–	147.5	146.5
$^{3}J_{H\text{-}H}$					
H5-H6R(M)	–	7.6	10.6	–	10.5
H5-H6S(M)	–	2.7	0.8	–	0.7
H5-H6R(M′)	–	–	–	10.4	10.6
H5-H6S(M′)	–	–	–	0.6	1.0
$^{3}J_{C\text{-}H}$					
C4-H1(M′M)	3.4	–	3.6	2.2	3.2
C1-H4(MM′)	4.6	–	4.4	5.3	5.0
C6-H1(MG1)	–	3.3	3.1	–	3.3
C6-H1(M′G2)	–	–	–	3.1	3.0
C1-H6R(G1M)	–	2.3	4.4	–	2.2
C1-H6S(G1M)	–	1.7	2.1	–	1.8
C1-H6R(G2M′)	–	–	–	2.2	3.5
C1-H6S(G2M′)	–	–	–	1.9	2.5

1:0) and those with a substitution level of (5:1) to the idealized homo-galactomannan (1:1). The galactosyl side groups were inserted onto the mannan backbone at random. Various computed average properties: C_X, L_X, $\langle R\rangle$ and $\langle s^2\rangle^{1/2}$ as functions of the degree of polymerization are shown in Fig. 8. Table 3 shows C_∞ and '*a*' estimated from the asymptotic behaviour of C_X and L_X.

Our results indicate that the insertion of galactosyl side chains induces an important lowering of the calculated chain extension when compared with that of pure mannan chains. The estimated asymptotic limit C_∞ of a pure mannan chain is 47 and this value decreases to 35 when the chain is substituted in the ratio of one side chain for each five skeletal units (5:1). However, at high levels of substitution (between 3:1 and 1:1), C_∞ values reach a limit in the chain contraction of about 30, showing that in this range the influence of galactose is not significant. Note that all the curves converge to their asymptotic values at low degrees of polymerization. This feature is independent of the degree of substitution and suggests a significant stiffness in these chains.

To investigate how the side chain distribution influences the galactomannan chain properties, calculations have been carried out for (2:1) and (3:1) Man:Gal ratios with the three possible extreme patterns of galactosyl distribution: random, block and alternated. Both ratios show the same trends, therefore only the results of the (2:1) Man:Gal ratio are shown in Fig. 9. For the same Man:Gal ratio, the distribution of galactosyl groups has a significant effect on the calculated features: the block polymer is predicted to be the stiffer one, whereas the alternating sequence is the most flexible. Random distributions are in between these two extremes.

Fig. 10 shows a drawing of a typical conformation of a segment (100 mannoses) of a mannan chain (a) and a galactomannan chain (b) having a random distribution of galactoses for a 2:1 Man:Gal ratio. Representative snapshots of 2:1 galactomannans (having 2000 main-chain residues) differing in the distribution of galactoses are shown in Fig. 11. These drawings were selected as representative examples from a survey of 4000 chain conformations from the MMC sample of chains having 3000 residues on the backbone.

Light scattering and viscometry are the principal techniques which have been used to characterize the size and

Table 3
Characteristic ratio C_∞ and persistence length '*a*' estimated from asymptotic behaviour of C_X and L_X

Polymer	C_∞	*a* (Å)
1:1 Galactomannan	30	96
2:1 Galactomannan	29	85
3:1 Galactomannan	31	91
4:1 Galactomannan	33	100
5:1 Galactomannan	37	113
Mannan	48	145

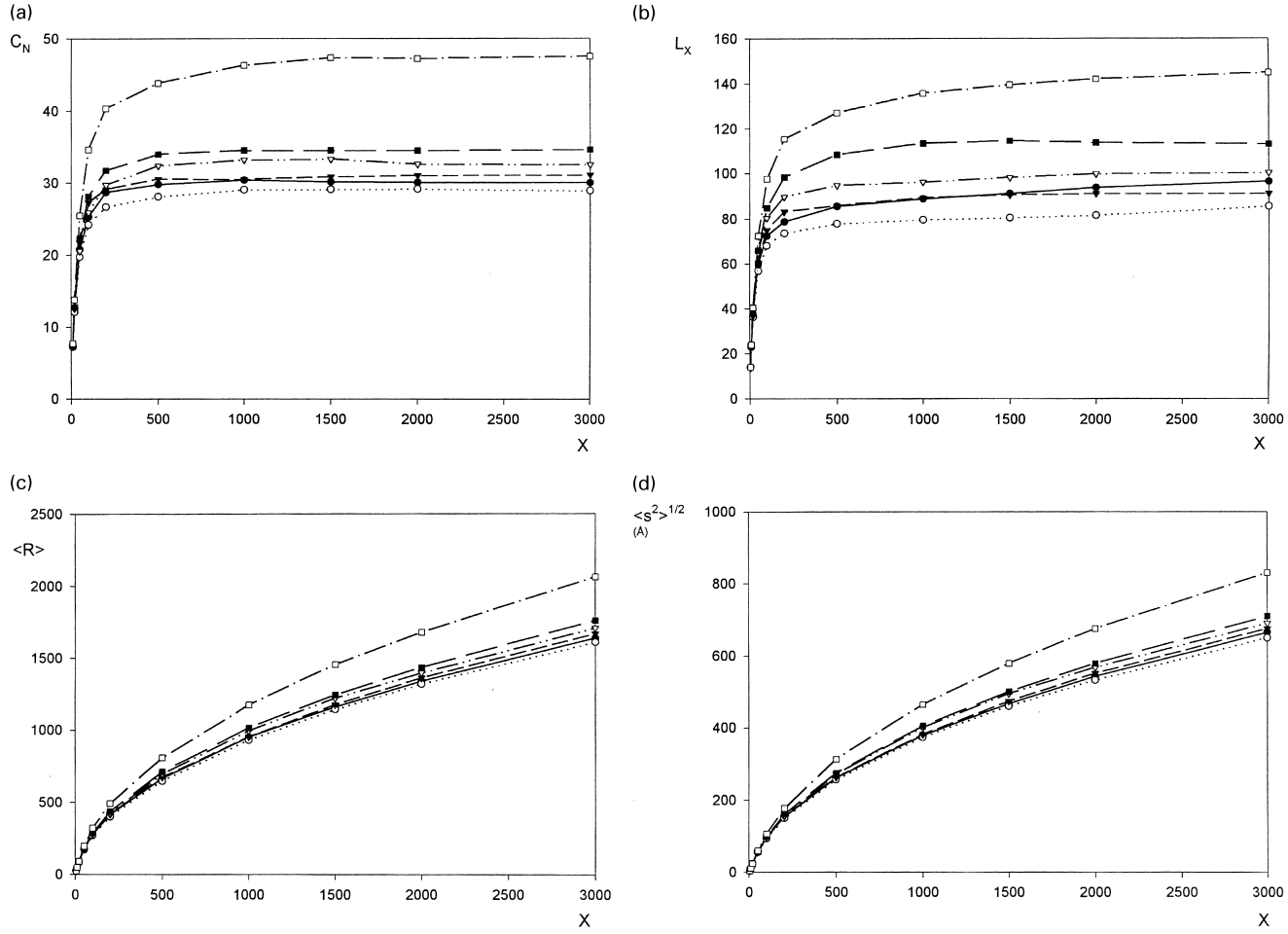

Fig. 8. Characteristic ratio C_N (a), persistence length L_X (b), end-to-end distance $\langle R \rangle$ (c) and radius of gyration $\langle s^2 \rangle^{1/2}$ (d) versus degree of polymerization calculated for mannan chains having different content of galactose substituents: Man:Gal ratios of 1:0 (□), 1:1 (●), 2:1 (○), 3:1 (▼), 4:1 (▽) and 5:1 (■).

shape of galactomannans. Experimental values of the squared radius of gyration are reported for galactomannans differing in their degree of substitution. The studied samples were those from *Mimosa scabrella*, *Cyamopsis tetragonoloba* (guar), *Schizolobium amazonicum* and *Ceratonia siliqua* (locust bean), having Man:Gal ratios of 1:1, 2:1, 3:1 and 4:1, respectively.

Galactomannan from *Mimosa scabrella* seeds, for which each mannose is substituted by a galactosyl group, have been extensively studied both experimentally and theoretically (Petkowicz et al., 1997). Fractions purified using gel permeation chromatography enables characterization of samples with homogeneous average molecular weights ranging from 3240 to 972 000. The excellent agreement between predicted values of the $\langle s^2 \rangle^{1/2}$ and '*a*' and the experimental ones suggests that the methods used in these studies successfully describe the solution behaviour of such chains. However, this is an extreme case in which the primary structure is unambiguously defined. For the other cases, ^{13}C NMR and specific degradation methods have been used to study the distribution of the galactosyl groups. These techniques suffer from limitations; only the nearest-neighbour and the next nearest-neighbour frequencies are determined and the true structure remains unknown. Therefore, in the present study, the three different schemes of galactosyl substitution onto the mannan backbone enables the generation of idealized primary structures which approximate the real ones. The literature data on 2:1, 3:1 and 4:1 galactomannans report experimental values for samples having unique average molecular weights of $1.3\,10^6$, $1.1\,10^6$ and $1.4\,10^6$, respectively, corresponding to 5350, 5000 and 7000 mannosyl backbone residues. To facilitate the comparison, specific MMC calculations of these galactomannan chains have been carried out within the three different schemes of galactosyl distribution.

Experimental measurement of the average squared radius of gyration $\langle s^2 \rangle^{1/2}$ for a sample of guar, with $M_W = 1.3\,10^6$, was 978 Å (Frollini et al., 1995). Guar galactomannans are characterized by a 2:1 composition. There is a good concordance between this value and the predicted one within the block pattern of substitution, that is 890 Å. Random and alternate patterns predict 841 Å and 750 Å, respectively. According to studies on the fine structure of

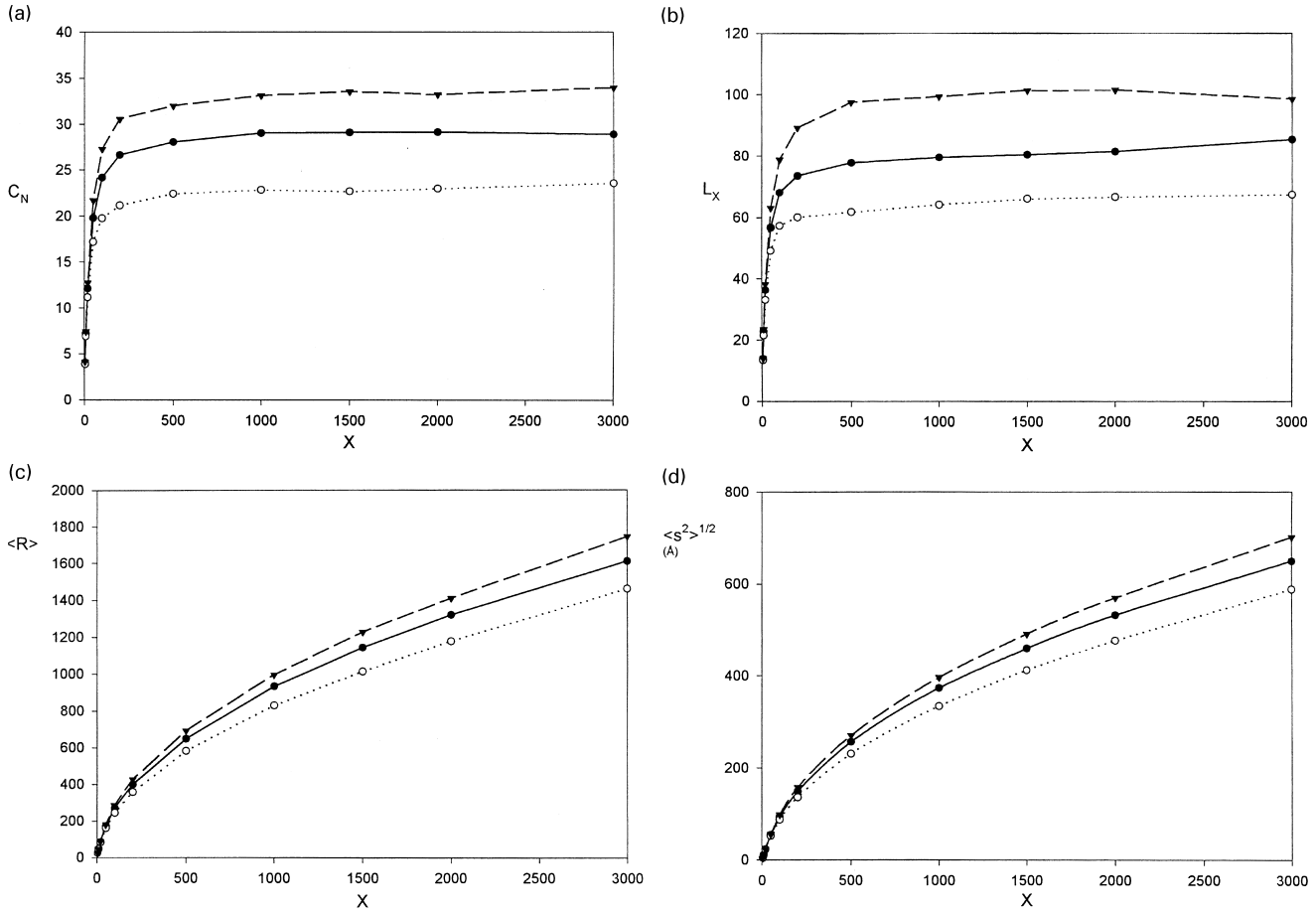

Fig. 9. Characteristic ratio C_N (a), persistence length L_X (b), end-to-end distance $\langle R \rangle$ (c) and radius of gyration $\langle s^2 \rangle^{1/2}$ (d) versus degree of polymerization calculated for a 2:1 galactomannan with different patterns of galactose distribution: random (●), blocks (▼) and alternate (○).

guar galactomannan by Hall & Yalpani (1980), D-galactosyl groups occur in blocks. However, other studies have suggested that the side chains are arranged mainly in pairs and triplets (Hoffman & Svensson, 1978, McCleary et al., 1985). There is a strong discrepancy in the reported experimental values of C_∞ that have been deduced from guar galactomannan. Published values range from 12.6 (Robinson et al., 1982) to 78–138 (Yalpani, 1988). The predicted value here was ~29. Another study of a 3:1 galactomannan ($M_w = 1.1\,10^6$) extracted from the seeds of *Schizolobium amazonicum* found a radius of gyration of 839 Å (Petkowicz, unpublished results). The predicted values were 826 Å, 750 Å and 890 Å for a random, alternate and block distribution of the galactosyl groups, respectively. There is quite good agreement between experimental data and those predicted for a random chain. Studies of its fine structure suggest that *Schizolobium amazonicum* galactomannan have a random arrangement of D-galactosyl groups (Ganter et al., 1995). An experimental radius of gyration value of 1450 Å, determined from a sample of 4:1 locust bean galactomannan with $M_W = 1.4\,10^6$ (Yalpani, 1988), is higher than our predicted value, 990 Å, for a random chain with the same Man:Gal ratio and M_W. Theoretical values for an alternate and a block distribution of side chains are 969 Å and 1072 Å, respectively.

4. Conclusion

Using molecular modelling techniques, the Φ, Ψ conformational properties of four representative fragments of galactomannan molecules, M_2, G^1M_2, G^2M_2 and $G^{1,2}M_2$ have been studied. Differences in the potential energy surfaces reflected the effect of the galactosyl substitution on the inherent flexibility of the mannobiosyl backbone. These surfaces allowed the Monte Carlo simulation of long galactomannan chains. The calculated mean characteristic ratio, squared radius of gyration, end-to-end distance and persistence length as a function of degree of polymerization have been discussed for various degrees and schemes of galactosyl substitution. It has been shown that the unperturbed dimensions are affected by both the degree of substitution and by the primary sequence of the molecule. Such a study has allowed a quantitative correlation to be drawn between

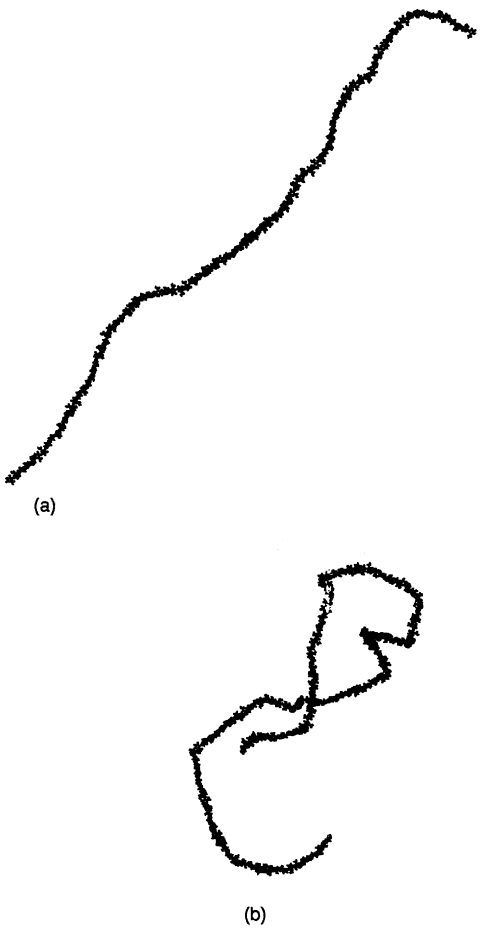

Fig. 10. Snapshots of a segment (100 mannosyl residues) of a mannan chain (a) and a random 2:1 galactomannan (b).

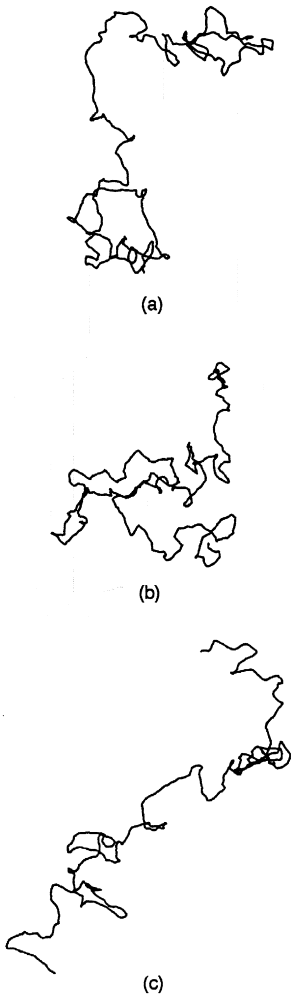

Fig. 11. Snapshots of galactomannans having 2000 mannosyl residues for different patterns of substitution: random (a), alternate (b) and blocks (c).

these two factors and the stiffness and extension of polymeric chains.

The concordance between the calculated and available experimental results suggests that both the methods and the strategy used to model galactomannans correctly describe the conformational behaviour of such chains.

Acknowledgements

C.L.O.P. is grateful to the Conselho Nacional de Desenvolvimento Cientifico e Tecnologico (CNPq) of Brazil for financial support during her stay at CERMAV.

References

Ahuja, M., & Rai, A. K. (1997). Adsorption studies with some chelating ion exchange resins derived from guaran. *Carbohydr. Polym., 33*, 57–62.

Allinger, N. L., Yuh, Y. H., & Lii, J.-H. (1989). Molecular mechanics. The MM3 force field for hydrocarbons. 1. *J. Am. Chem. Soc., 111*, 8551–8566.

Allinger, N. L., Zhu, Z. S., & Chen, K. J. (1992). Molecular mechanics (MM3) studies of carboxylic acids and esters. *J. Am. Chem. Soc., 114*, 6120–6133.

Bergamini, J.-F., Boisset, C., Mazeau, K., Heyraud, A., & Taravel, F. R. (1995). Conformational behaviour of oligo-galactomannan chains inferred from NMR spectroscopy and molecular modelling. *New J. Chem., 19*, 115–127.

Boutherin, B., Mazeau, K., & Tvaroska, I. (1997). Conformational statistics of pectin substances in solution by a Metropolis Monte Carlo study. *Carbohydr. Polym., 32*, 255–266.

Craig, D. Q. M., Kee, A., Tamburic, S., & Barnes, D. (1997). An investigation into the temperature dependence of the rheological synergy between xanthan gum and locust bean gum mixtures. *J. of Biomaterials Science, 8*, 377–389.

Dowd, M. K., French, A. D., & Reilly, P. J. (1992). Conformational analysis of the anomeric forms of sophorose, laminarabiose, and cellobiose using MM3. *Carbohydr. Res., 233*, 15–34.

Dowd, M. K., Reilly, P. J., & French, A. D. (1993). Molecular modelling of two disaccharides containing fructopyranose linked to glucopyranose. *J. Carbohydr. Chem., 12*, 449–457.

Dowd, M. K., Reilly, P. J., & French, A. D. (1994). Relaxed-residue

conformational mapping of the three linkage bonds of isomaltose and gentiobiose with MM3(92). *Biopolymers, 34*, 625–638.

Dowd, M. K., French, A. D., & Reilly, P. J. (1995). Molecular mechanics modelling of α-(1 → 2)-, α-(1 → 3)-, and α-(1 → 6)-linked mannosyl disaccharides with MM3(92). *J. Carbohydr. Chem., 14*, 589–600.

French, A. D. (1989). Comparisons of rigid and relaxed conformational maps for cellobiose and maltose. *Carbohydr. Res., 188*, 206–211.

French, A. D., Dowd, M. K., & Reilly, P. J. (1997). MM3 modelling of fructose ring shapes and hydrogen bonding. *J. Mol. Struct. (Theochem), 395-396*, 271–287.

Frollini, E., Reed, W. F., Milas, M., & Rinaudo, M. (1995). Polyelectrolytes from polysaccharides: selective oxidation of guar gum—a revisited reaction. *Carbohydr. Polym., 27*, 129–135.

Ganter, J. L. M. S., Heyraud, A., Petkowicz, C. L. O., Rinaudo, M., & Reicher, F. (1995). Galactomannans from Brazilian seeds: characterization of the oligosaccharides produced by mild acid hydrolysis. *Int. J. Biol. Macromol., 17*, 13–19.

Garnier, C., Schorsch, C., & Doublier, J.-L. (1995). Phase separation in dextran/locust bean gum mixtures. *Carbohydr. Polym., 28*, 313–317.

Grasdalen, H., & Painter, T. (1980). NMR studies of composition and sequence in legume-seed galactomannans. *Carbohydr. Res., 81*, 59–66.

Haasnoot, C. A. G., De Leeuw, F. A. A. M., & Altona, C. (1980). The relationship between proton–proton NMR coupling constants and substituent electronegatives—I. An empirical generalization of the Karplus equation. *Tetrahedron, 36*, 2783–2792.

Hall, L. D., & Yalpani, M. (1980). A high-yielding, specific method for the chemical derivatization of D-galactose-containing polysaccharides: oxidation with D-galactose oxidase, followed by reductive amination. *Carbohydr. Res., 81*, C10–C12.

Hoffman, J., & Svensson, S. (1978). Studies of the distribution of the D-galactosyl side-chains in guaran. *Carbohydr. Res., 65*, 65–71.

IUPAC—Macromolecular Division—Commission on Macromolecular Nomenclature (1989). Definitions of terms relating to individual macromolecules, their assemblies, and dilute polymer solutions. (Recommendations 1988). *Pure and Appl. Chem., 61*, 211–241.

IUPAC–IUB Joint Commission on Biochemical Nomenclature (1997). Nomenclature of Carbohydrates (Recommendations 1996). *Carbohydr. Res., 297*, 1–92.

Izydorczyk, M. S., & Biliaderis, C. G. (1996). Gradient ammonium sulphate fractionation of galatomannans. *Food Hydrocolloids, 10*, 295–300.

Jimenez-Barbero, J., Noble, O., & Pfeffer, C. (1988). Solvent-specific energy surfaces of carbohydrates: the mannobiose case. *New J. Chem., 12*, 941–946.

Lapasin, R., De Lorenzi, L., Pricl, S., & Torriano, G. (1995). Flow properties of hydroxypropyl guar gum and its long-chain hydrophobic derivatives. *Carbohydr. Polym., 28*, 195–202.

Marchessault, R. H., & Perez, S. (1979). Conformations of the hydroxymethyl group in crystalline aldohexopyranoses. *Biopolymers, 18*, 2369–2374.

McCleary, B. V., Clarck, A. H., Dea, I. C., & Rees, D. A. (1985). The fine structures of carob and guar galactomannans. *Carbohydr. Res., 139*, 237–260.

Metropolis, N., Rosenbluth, A. W., Rosenbluth, M. N., Teller, A. H., & Teller, E. (1953). Equation of state calculations by fast computing machines. *J. Chem. Phys., 21*, 1087–1092.

Painter, T. J., Gonzalez, J. J., & Hemmer, P. C. (1979). The distribution of D-galactosyl groups in guaran and locust-bean gum: new evidence from periodate oxidation. *Carbohydr. Res., 69*, 217–226.

Petkowicz, C. L. O., Milas, M., Mazeau, K., Bresolin, T., Ganter, J. L. M. S., Reicher, F., & Rinaudo, M. (1997). Conformation of galactomannan. Experimental and modelling approaches. *Int. J. Biol. Macromol*, submitted.

Reid, J. S. G., & Edwards, M. E. (1995). In A. M. Stephen (Ed.), *Food Polysaccharides and their Applications*. New York: Marcel Dekker (pp. 155–186).

Robinson, G., Ross-Murphy, S. B., & Morris, E. R. (1982). Viscosity-molecular weight relationships, intrinsic chain flexibility, and dynamic solution properties of guar galactomannan. *Carbohydr. Res., 107*, 17–32.

Sheldrick, B., Mackie, W., & Akrigg, D. (1984). The crystal and molecular structure of *O*-β-D-mannopyranosyl-(1 → 4)-α-D-mannopyranose (mannobiose). *Carbohydr. Res., 132*, 1–6.

Sudhakar, V., Singhal, R. S., & Kulkarni, P. R. (1996). Effect of salts on interactions of starch with guar gum. *Food Hydrocolloids, 10*, 329–334.

Taravel, F. R., Mazeau, K., & Tvaroska, I. (1995). Conformational analysis of carbohydrate inferred from NMR spectroscopy and molecular modelling. Applications to the behaviour of oligo-galactomannan chains. *Braz. J. of Med. and Biol. Res., 28*, 723–732.

Tvaroska, I., & Kozar, T. (1980). Theoretical studies on the conformation of saccharides. 3. Conformational properties of the glycosidic linkage in solution and their relation to the anomeric and exoanomeric effects. *J. Am. Chem. Soc., 102*, 6929–6936.

Tvaroska, I., Perez, S., Noble, O., & Taravel, F. (1987). Solvent effect on the stability of mannobiose conformers. *Biopolymers, 26*, 1499–1508.

Tvaroska, I., Hricovini, M., & Petrakova, E. (1989). An attempt to derive a new Karplus-type equation of vicinal proton–carbon coupling constants for C-O-C-H segments of bonded atoms. *Carbohydr. Res., 189*, 359–362.

Tvaroska, I., & Taravel, F. R. (1991). One-bond carbon–proton coupling constants: angular dependence in α-linked oligosaccharides. *Carbohydr. Res., 221*, 83–94.

Tvaroska, I., & Taravel, F. R. (1992). One-bond carbon–proton coupling constants: angular dependence in β-linked oligosaccharides. *J. Biomol. NMR, 2*, 421–430.

Viebke, C., & Piculell, L. (1996). Adsorption of galactomannans onto agarose. *Carbohydr. Polym., 29*, 1–5.

Yalpani, M. (1988). *Polysaccharides. Syntheses, Modifications and Structure/Property Relations. Studies in Organic Chemistry*, Vol. 36. Amsterdam: Elsevier (pp. 83–141).